Flow Regimes of the Three-Phase Circulating Fluidized Bed

W. G. Liang, Q. W. Wu, Z. Q. Yu, Y. Jin, and H. T. Bi
Fluidization Lab., Dept. of Chemical Engineering, Tsinghua University, Beijing, Peoples Republic of China 100084

Gas-solids circulating fluidized beds have been successfully used in catalytic cracking of heavy oil, coal combustion, and some metallurgical and physical processes (Grace, 1990). Gas-liquid-solids fluidized beds are operated mainly in conventional fluidization regimes without solids circulation or in the transport regime with low solids holdups (less than 5%) (Fan, 1989). A circulating/fast fluidization regime, however, has not been studied. A three-phase circulating fluidized bed has several potential applications in biochemical and chemical processes. Three-phase fluidized-bed bioreactors generally use light and small particles (Berk et al., 1984). Circulating operation can promote solids mixing and increase product throughput per unit bed cross section, while high shear stress can promote biofilm renewal (Pirozzi et al., 1990). In three-phase hydrotreating reactors, solids catalysts lose their activity due to the deposit of metal and coke on the surface. Circulating operation not only regenerates deactivated catalyst continuously using accompanying downcomers but also transfers heat to and from the reactor. This article discusses the flow regimes of the three-phase circulating fluidized bed.

Experimental Studies

The experimental apparatus is shown in Figure 1. The riser is 140-mm-dia., 3-m-high Plexiglas. Tap water and air were used as liquid and gas phases, respectively. Glass beads of 0.405 mm in mean diameter and density 2,460 kg/m^3 were used as the solid phase. In the operation, fluidizing water was introduced from the base of the riser through a liquid distributor, while solids flow rate was regulated by a secondary water flow from a side port near the bottom of the riser. The superficial liquid velocity was calculated based on the total flow rate from both the liquid distributor and the secondary side port. Gas was introduced separately through a gas distributor located well above the bottom liquid distributor. Well-mixed three-phase flow was achieved in the test section above the gas distributor. Solids entrained from the top of the riser was separated from the water and returned to a reservoir. The solids circulation rate was determined by measuring the amount of particles collected in a metering tank on the top of the standpipe after the butterfly valve beneath the metering tank was closed, similar to the method used in the gas-solids circulating fluidized bed (Burkell et al., 1988).

Local gas holdup was measured using an electrical conductivity probe. The tip of the probe was a 0.1-mm platinum wire, covered by a 0.2-mm glass tube. The probe was installed with the tip directed downward to minimize the disturbance of local flow patterns. Typical signals from the probe are shown in Figure 2. The output voltage is seen to drop sharply when bubbles pass the probe. The local bubble fraction can thus be determined by:

$$\epsilon_g = \Sigma t_i / T \tag{1}$$

where t_i is the exposure time of the probe to bubbles and T is the total record time. The cross-sectional average gas holdup is calculated by:

$$\bar{\epsilon}_g = \frac{2}{R^2} \int_0^R \epsilon_g r dr \tag{2}$$

To evaluate the cross-sectional average solids holdup, pressure drops across the test section were also measured. The sectional average solids holdup is evaluated by combining Eqs. 2, 3 and 4:

$$-dP/dz = \rho_g \bar{\epsilon}_g + \rho_l \bar{\epsilon}_l + \rho_s \bar{\epsilon}_s \tag{3}$$

Correspondence concerning this article should be addressed to Y. Jin.

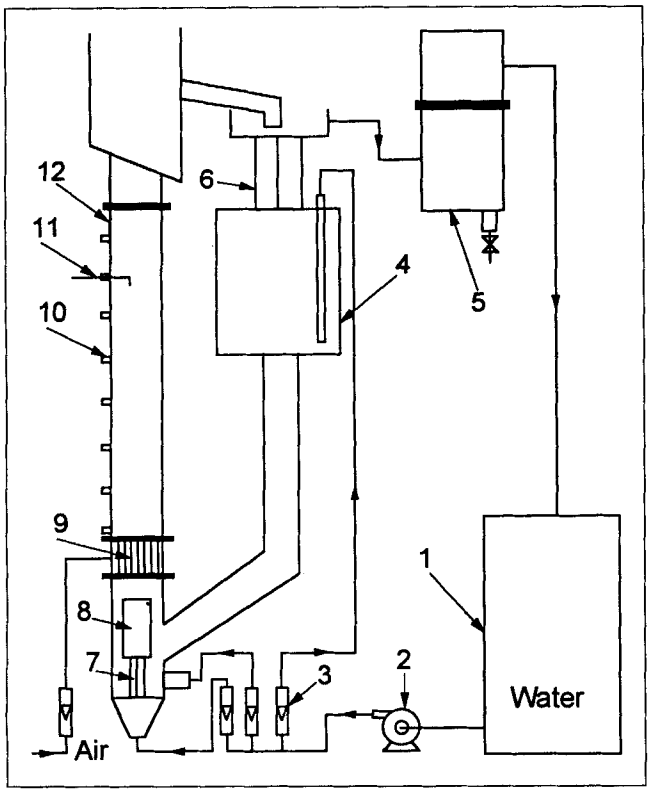

Figure 1. Three-phase circulating bed.

(1) Liquid reservoir; (2) liquid pump; (3) flowmeters; (4) particle reservoir; (5) secondary liquid-solid separator; (6) particle metering tank; (7) primary liquid distributor; (8) liquid distributor; (9) gas distributor; (10) manometer tap; (11) test section.

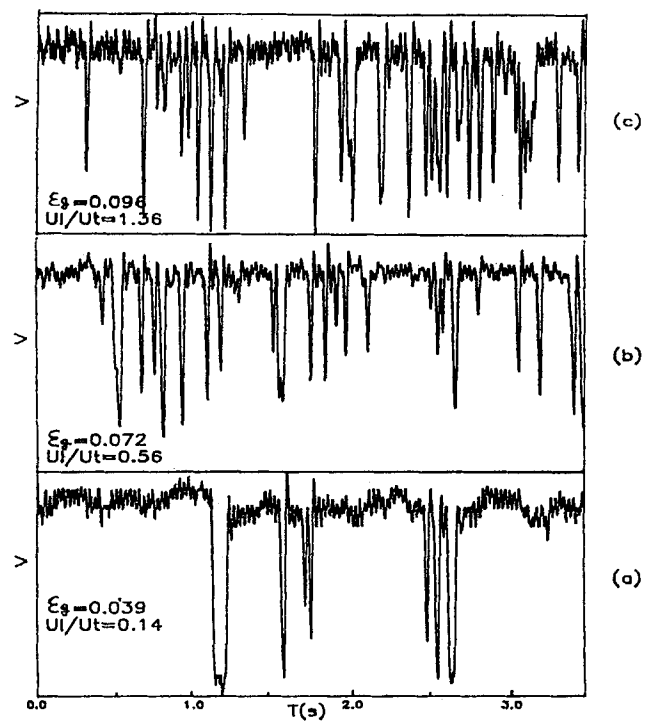

Figure 2. Typical signals from conductivity probe at three superficial liquid velocities.

$U_g = 0.036$ m/s and $r/R = 0.5$.

$$\bar{\epsilon}_g + \bar{\epsilon}_l + \bar{\epsilon}_s = 1 \quad (4)$$

Before it was used for three-phase measurement, the probe was calibrated in a gas-liquid bubble column by comparing cross-sectional average gas holdups from both the pressure drop measurement and the conductivity probe measurement corresponding to the same level.

Results and Discussion

A three-phase circulating fluidized bed can be considered as a combination of the gas-liquid bubbly flow and the liquid-solids vertical transport. In the gas-liquid bubbly flow, bubbles become smaller with increasing liquid velocity and the flow pattern is said to transform from coalescing to dispersed bubble flow regimes (Fan, 1989). Bubbles in three-phase circulating fluidized beds with high liquid velocities are thus expected to be smaller and distributed more uniformly. This is evidenced from Figures 2a, 2b and 2c where the number of bubbles is seen to increase with increasing liquid flow rate at a given superficial gas velocity and solids circulation rate; while the bubble size decreases leading to the increase in gas holdups. The transition from coalescing to dispersed bubble flow regimes can thus be considered to occur when the bubble frequency or the gas holdup starts to increase sharply with increasing superficial liquid velocity.

In gas-solids circulating fluidized beds, the onset of circulating operation is marked by the significant carryover of particles from the top of the riser (Yerushalmi and Cankurt, 1979). The velocity at which solids are carried over significantly has been found to be much higher than the terminal velocity of single particles in risers with fine particles because fine particles tend to stick together by interparticle forces (Yerushalmi et al., 1978; Bi and Fan, 1992). Liquid-solids and gas-liquid-solids circulating fluidized beds are characterized by the continuous feeding and carryover of solids phase; the onset of circulating operation can therefore be marked by the significant carryover of particles. Figure 3 shows pressure drops measured at two locations with one right above the gas distributor and the other near the top of the riser as a function of superficial liquid

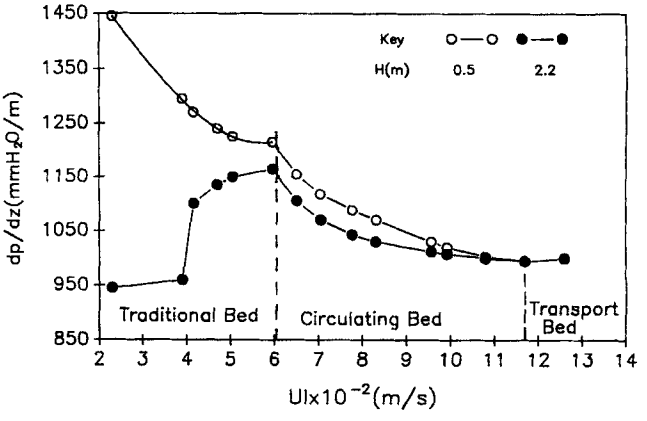

Figure 3. Pressure drops at lower and upper sections of the riser as a function of superficial liquid velocity.

$U_g = 0.018$ m/s and $U_l = 0.011$ m/s.

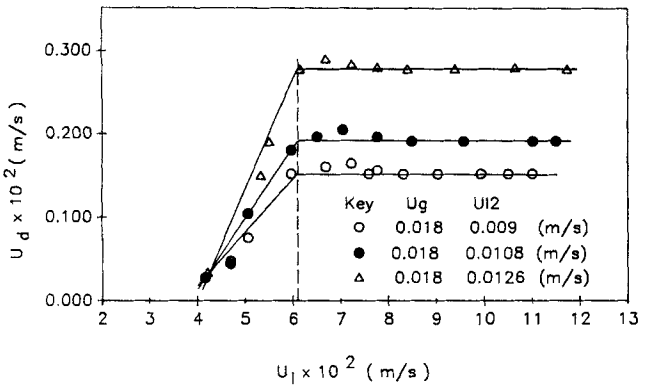

Figure 4. Solids circulation rate as a function of superficial liquid velocity at given secondary liquid flow rate.

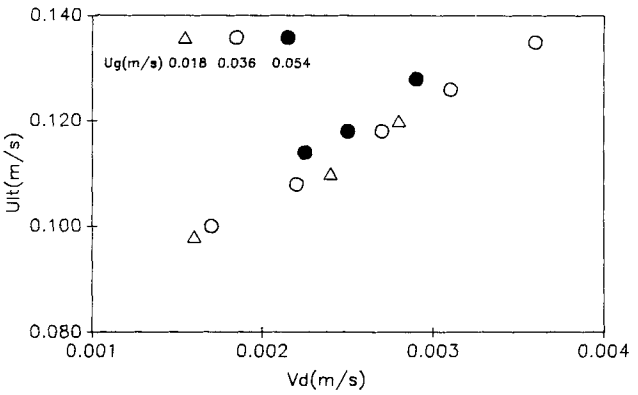

Figure 6. Effect of superficial gas velocity on solids circulation rate on transition velocity U_{lt}.

velocity with the secondary liquid flow rate fixed at a constant. It is seen that pressure drop in the lower region continues to decrease with increasing liquid flow rate due to bed expansion (note that solids phase is heavier than the liquid phase). In the upper region, pressure drop does not change much until the superficial liquid velocity exceeds 40 mm/s, indicating that particles have been entrained to the top section due to dense-phase expansion. Solids carryover was observed when superficial liquid velocity approaches the terminal velocity of single particles ($U_t = 53$ mm/s). Beyond this point, solids continue to be entrained and the column will be emptied of particles quickly if no particles are fed back to the bottom of the riser. Therefore, the terminal velocity of single particles can be safely taken as the lowest limit of the superficial liquid velocity required for the circulating operation of three-phase fluidized beds.

With further increase of superficial liquid velocity to about 61 mm/s, solids circulation rate reaches a constant with a superficial particle velocity of around 2.0 mm/s. This is seen more clearly from Figure 4 where the solids circulation rate is plotted vs. superficial liquid velocity. Beyond this velocity, the pressure gradient at the lower section is still higher than that at the upper section, indicating higher solids concentration at the lower section. When superficial liquid velocity is increased further beyond 61 mm/s, pressure gradient at the upper section starts to drop off, because solids concentration decreases with increasing superficial liquid velocity at a constant solids circulation rate. Eventually, pressure gradients at both the upper and lower sections merge together when superficial liquid velocity exceeds 117 mm/s, indicating that solids become uniformly distributed along the riser.

In gas-solids circulating beds, the termination of fast fluidization regime to the pneumatic transport has been considered to commonly occur when solids become uniformly distributed along the riser with increasing gas velocity at a given solids circulation rate (Takeuchi et al., 1986; Bi et al., 1993). Similarly, the termination of three-phase circulating fluidization to three-phase transport can be defined by the velocity, U_{lt}, at which axial solids segregation disappears from the riser with increasing superficial liquid velocity at given solids circulation rate and superficial gas velocity as shown in Figure 3.

Another boundary is the lower limit of stable operation of three-phase circulating fluidized beds. It has been revealed in gas-solids circulating beds that there exists a maximum solids circulation rate for a given superficial gas velocity beyond which stable operation becomes impossible due to further increase in solids circulation rate being prevented by inappro-

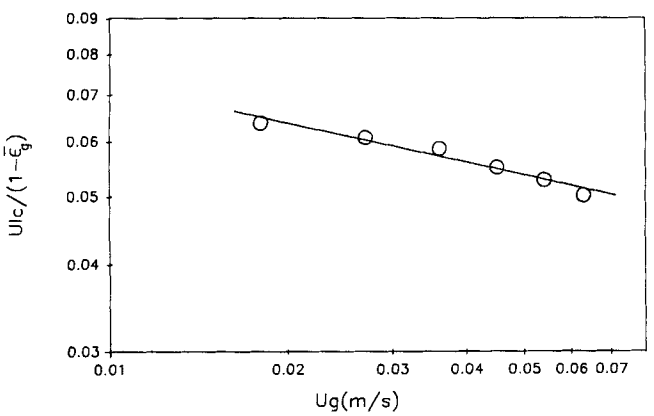

Figure 5. Effect of superficial gas velocity on transition velocity U_{lc}.

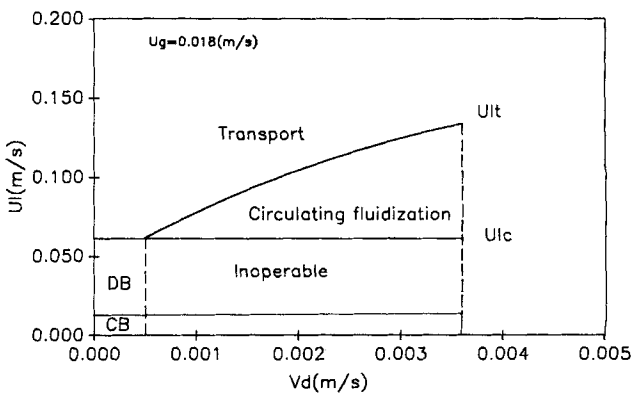

Figure 7. Flow regimes of air-water-0.405-mm glass beads circulating fluidized bed.

$U_g = 0.018$ m/s.

CB: coalescing bubble flow; DB: Dispersed bubble flow.

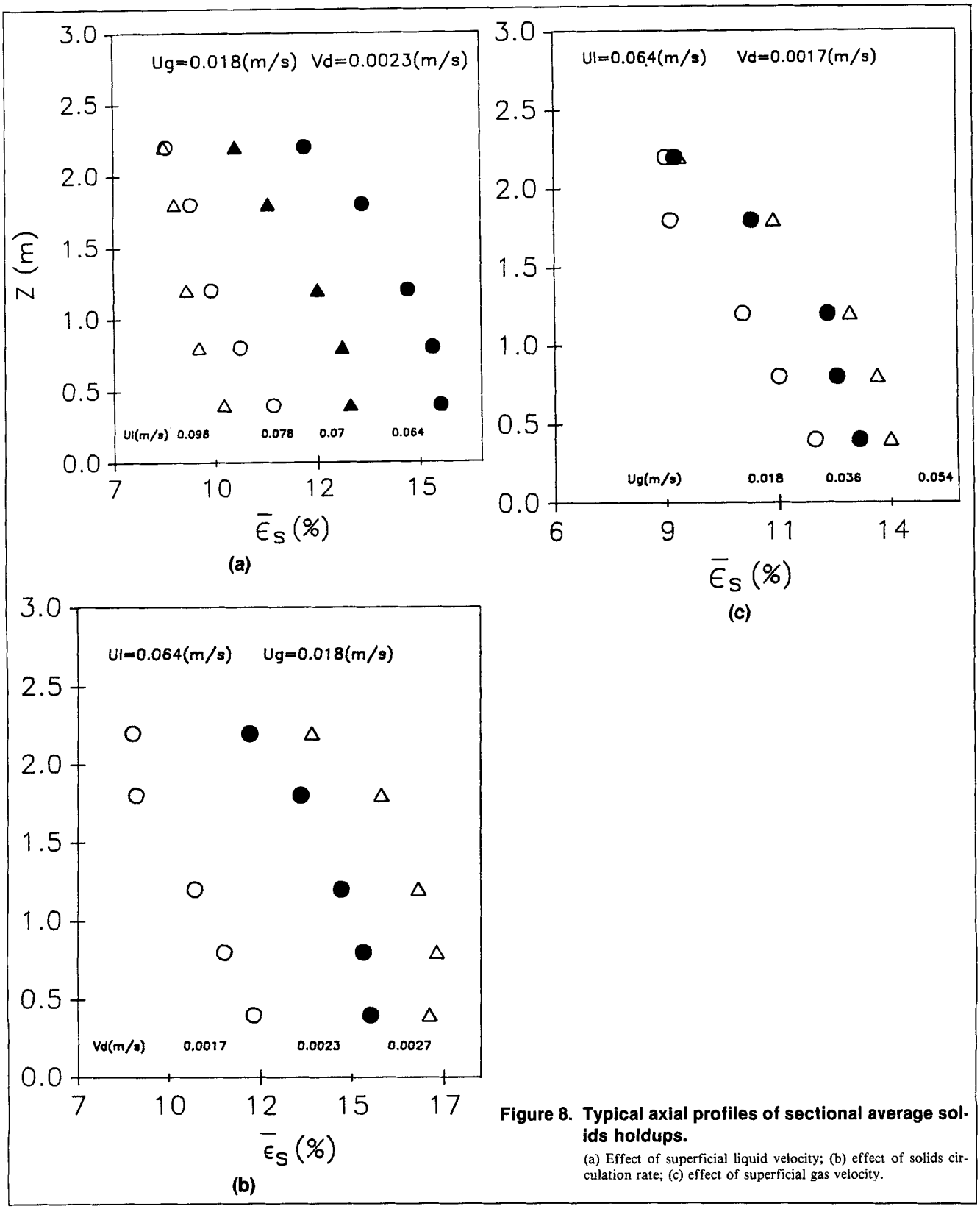

Figure 8. Typical axial profiles of sectional average solids holdups.

(a) Effect of superficial liquid velocity; (b) effect of solids circulation rate; (c) effect of superficial gas velocity.

priate pressure balance in the whole unit (Takeuchi et al., 1986; Bi and Zhu, 1993). Such a transition in three-phase circulating fluidized bed can be determined by plotting solids circulation rate vs. superficial liquid velocity at constant gas flow rate and secondary liquid flow rate. It is seen in Figure 4 that stable operation at a constant solids circulation rate can be maintained at high liquid flow rates. However, solids circulation rate starts to drop off when liquid flow rate is reduced to a certain point, U_{lc}, due to the reduction in the solids-carrying-capacity of the liquid. U_{lc} thus corresponds to the minimum

velocity required to maintain stable operation of the riser at a constant solids circulation rate.

Both U_{lt} and U_{lc} are functions of the superficial gas velocity. Figure 4 shows that U_{lc} is almost independent of solids circulation rate within the range of this study, while U_{lc} in Figure 5 tends to decrease with increasing superficial gas velocity, because the presence of gas bubbles increases the interstitial liquid velocity and promotes particle entrainment. Figure 6 shows that the transition velocity, U_{lt}, is also a function of solids circulation rate and superficial gas velocity, although the effect of superficial gas velocity appears to be trivial within the range tested.

Based on all the above information, a flow regime map is proposed for the three-phase circulating fluidized bed with air, water, and 0.405 mm glass beads. As shown in Figure 7, the circulating/fast fluidization regime is bounded by the onset velocity, U_{lc}, and the transition velocity, U_{lt}. Beyond U_{lt} lies the transport regime, which is characterized by the uniform axial distribution of solids holdups. While the region with solids circulation rate higher than V_{dmin} and superficial liquid velocity lower than U_{lc} is inoperable due to the buildup of inappropriate pressure balance in the unit, this can be avoided by using a large standpipe, increasing solids inventory, or reducing resistance over the solids control valve (Bi and Zhu, 1993). A conventional three-phase fluidized bed is always operated below U_{lc} with solids entrainment rate smaller than V_{dmin}. Based on the bubble behavior, the flow pattern in conventional three-phase fluidized beds at low gas flow rate can further be divided into coalescing bubble flow and dispersed bubble flow regimes. To generalize the present proposed flow regime map, effects of gas, liquid and particle properties on U_{lc} and U_{lt} still need to be investigated by using different kinds of gas, liquid, and particles.

Figures 8a, 8b and 8c show typical axial solids concentration profiles. Similar to gas-solids circulating beds, S-shape axial profiles are present in the fast fluidization regime of three-phase circulating fluidized beds with a dense region at the bottom and a dilute region at the top. Such a dense bottom-lean top structure disappears when the superficial liquid velocity is increased to be higher than U_{lt} (see Figure 8a). It is also seen that solids holdup increases with increasing solids circulation rate (Figure 8b) and increases slightly with increasing superficial gas velocity at fixed superficial liquid velocity and solids circulation rate (Figure 8c). To understand the formation of such flow patterns in three-phase circulating fluidized beds, the local gas, liquid and solids flow structure still needs to be studied in the future.

Notation

P = pressure, Pa
r/R = radial ratio
U_g = superficial gas velocity, m/s
U_l = superficial liquid velocity based on total liquid flow rate, m/s
U_{lc} = onset velocity of three-phase circulating/fast fluidization, m/s
U_{lt} = transition velocity from three-phase circulating/fast fluidization to transport regimes, m/s
U_{l2} = superficial liquid velocity supplied from the side port for the regulation of solids circulation rate, m/s
U_t = terminal velocity of single particles in water, m/s
v = recorded output signals from the conductivity probe, V
V_d = superficial particle velocity, $(=G_s/\rho_s)$, m/s
V_{dmin} = minimum superficial particle velocity required for circulating operation, m/s
z = axial location, m

Greek letters

ϵ_g = local gas holdup
$\bar{\epsilon}_g$ = cross-sectional average gas holdup
$\bar{\epsilon}_l$ = cross-sectional average liquid holdup
$\bar{\epsilon}_s$ = cross-sectional average solids holdup
ρ_g = gas density, kg/m^3
ρ_l = liquid density, kg/m^3
ρ_s = solids density, kg/m^3

Literature Cited

Berk, D., L. A. Behie, A. Jones, B. H. Lesser, and G. M. Gaucher, "The Production of the Antibiotic Patulin in a Three-Phase Fluidized Bed Reactor: I. Effect of Medium Composition," *Can. J. Chem. Eng.*, **62**, 112 (1984).

Burkell, J. J., J. R. Grace, J. Zhao, and C. J. Lim, "Measurement of Solids Circulation Rates in Circulating Fluidized Beds," *Circulating Fluidized Bed Technology II*, P. Basu and J. F. Large, eds., Pergamon Press, Oxford, p. 501 (1988).

Bi, H. T., and L.-S. Fan, "On the Existence of Turbulent Regime in Gas-Solid Fluidization," *AIChE J.*, **38**, 297 (1992).

Bi, H. T., and J. Zhu, "Static Instability Analysis of Circulating Fluidized Beds and Concept of High-Density Risers," *AIChE J.*, **39**, 1272 (1993).

Bi, H. T., J. R. Grace, and J. Zhu, "On Types of Choking in Pneumatic Systems," *Int. J. Multiphase Flow*, **19**, 1077 (1993).

Fan, L. S., *Gas-Liquid-Solid Fluidization Engineering*, Butterworths (1989).

Grace, J. R., "High-Velocity Fluidized Bed Reactors," *Chem. Eng. Sci.*, **45**, 1953 (1990).

Pirozzi, D., L. Gianfreda, G. Greco, and L. Massimilla, "Development of a Circulating Fluidized Bed Fermentor: the Hydrodynamic Model for the System," *AIChE Symp. Ser.*, Vol. 85, No. 270, p. 101 (1989).

Takeuchi, H., T. Hirama, T. Chiba, J. Biswas, and L. S. Leung, "A Quantitative Regime Diagram for Fast Fluidization," *Powder Technol.*, **47**, 195 (1986).

Yerushalmi, J., and N. T. Cankurt, "Further Studies of the Regime of Fluidization," *Powder Technol.*, **24**, 187 (1979).

Manuscript received Oct. 5, 1993, and revision received Jan. 26, 1994.